

# Study on optical nonlinearity and optical limiting property of porphyrin-oxygenated carbon nanomaterial blends\*

WEN Hao (温浩)<sup>1,2</sup>, ZHANG Xiao-liang (张校亮)<sup>1,2,3,\*\*</sup>, LIU Zhi-bo (刘智波)<sup>3</sup>, YAN Xiao-qing (鄢小卿)<sup>3</sup>, LI Xiao-chun (李晓春)<sup>1,2</sup>, and TIAN Jian-guo (田建国)<sup>3</sup>

1. Key Laboratory of Advanced Transducers and Intelligent Control System, Ministry of Education, Taiyuan University of Technology, Taiyuan 030024, China

2. College of Physics and Optoelectronics, Taiyuan University of Technology, Taiyuan 030024, China

3. Key Laboratory of Weak Light Nonlinear Photonics, Ministry of Education, Teda Applied Physics School and School of Physics, Nankai University, Tianjin 300457, China

(Received 24 March 2015; Revised 14 April 2015)

©Tianjin University of Technology and Springer-Verlag Berlin Heidelberg 2015

Stable porphyrin-oxygenated carbon nanomaterial dispersions were prepared by blending porphyrin solutions with hydroxyl groups modified multi-walled carbon nanotubes (MWNTs-OH) and graphene oxide (GO) dispersions, respectively. Optical nonlinearity and optical limiting (OL) property of these blends are investigated in nanosecond regime. Results show that the OL performance of the blends can be tuned by changing the concentrations ratio of porphyrin and oxygenated carbon nanomaterials. The high concentration of oxygenated carbon nanomaterial leads to the poor OL performance. However, with the moderate concentration, the blends exhibit the low threshold value of OL and the enhanced OL performance at high fluence region. The superior OL performance can be attributed to complementary mechanisms and possible photoinduced electron or energy transfer between porphyrin moiety and oxygenated carbon nanomaterials.

**Document code:** A **Article ID:** 1673-1905(2015)03-0161-5

**DOI** 10.1007/s11801-015-5047-5

Materials with large optical nonlinearity and excellent optical limiting (OL) property can be promising candidates for optical limiters. Among various nonlinear optical materials<sup>[1-5]</sup>, porphyrins with large  $\pi$ -conjugated structures have shown excellent OL property at low fluence region due to strong reverse saturable absorption (RSA)<sup>[3]</sup>. However, this kind of materials usually exhibit poor OL performance at high fluence region due to thermal degradation and RSA saturation<sup>[6]</sup>. Carbon nanomaterials, including one-dimensional carbon nanotubes (CNTs) and two-dimensional graphene, have shown excellent broadband OL property at high fluence region due to strong nonlinear scattering (NLS), but the OL threshold of NLS is usually high<sup>[7,8]</sup>. What's more, pristine carbon nanomaterials usually exhibit poor dispersion in common solvents. To promote their OL performance and dispersion quality, RSA molecules-carbon nanomaterials composites were prepared, which show excellent OL performance due to the complementary mechanism of RSA, NLS and the possible photoinduced electron or energy transfer mechanism<sup>[9-12]</sup>.

Oxygenated derivatives of carbon nanomaterials, such as multi-walled carbon nanotubes with hydroxyl groups (MWNTs-OH) and graphene oxide (GO), exhibit better dispersion quality than pristine carbon nanomaterials which also show strong NLS and OL properties<sup>[13-15]</sup>. Blending RSA molecules with these oxygenated carbon nanomaterials may lead to stable blend system with tunable, even superior OL performance. In this paper, stable porphyrin-oxygenated carbon nanomaterial blends were prepared. The absorption, fluorescence spectrum, optical nonlinearity and OL property of the blends are studied. Results show that the optical nonlinearity and OL property of porphyrin can be tuned by adding MWNTs-OH and GO with different concentrations, respectively. Under moderate concentration, the two blends show low OL threshold and keep strong OL at high fluence region. No obvious nonlinear refraction signal is observed in these samples.

Free base tetraphenylporphyrin (TPP) was purchased from Sigma-Aldrich Co., LLC. MWNTs-OH with diameter of 20–30 nm was purchased from Chengdu Or-

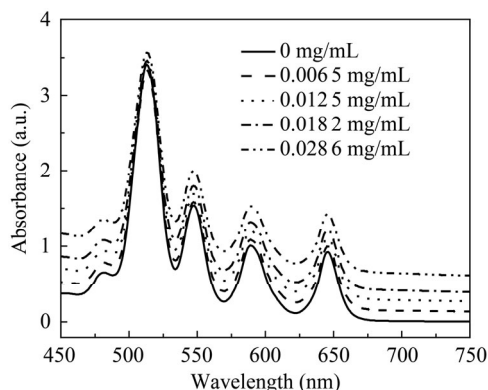
\* This work has been supported by the National Natural Science Foundation of China (No.61174010), the Shanxi International Cooperation Project (No.2012081043), the Shanxi Scholarship Council (No.2013-038), and the Scientific Research Starting Foundation from Taiyuan University of Technology (No.tyut-rc201162a).

\*\* E-mail: zhangxiaoliang@tyut.edu.cn

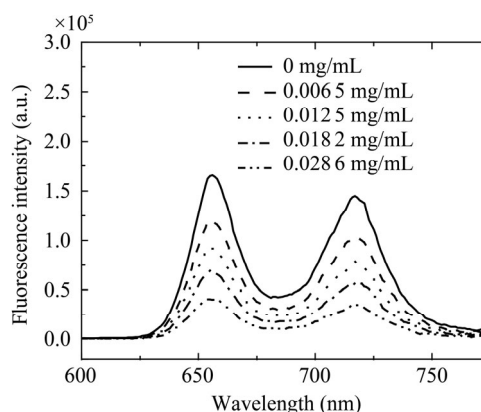
ganic Chemicals Co., Ltd., Chinese Academy of Sciences. GO was prepared by the modified hummer method<sup>[16]</sup>. TPP, MWNTs-OH and GO were dispersed in N,N-dimethylformamide (DMF) with initial concentrations of 0.32 mg/mL, 0.2 mg/mL and 1.0 mg/mL by sonicating for 1 h, respectively. MWNTs-OH (or GO) dispersions and TPP solutions were then mixed, and then diluted to the desired concentrations for experiments. All the dispersions were poured into 5 mm quartz cells.

Optical nonlinearities of the samples were measured by open-aperture Z-scan technique<sup>[17]</sup>. In Z-scan measurements, a Q-switched Nd:YAG laser (Continuum Surelite-II) was used to generate 5 ns pulses at 532 nm with repetition rate of 10 Hz. The beam waist was about 23  $\mu\text{m}$  at focus. For the measurements of OL and NLS properties, the single pulse mode was used, the samples were fixed near the focus, and the experimental configuration is the same as that in Refs.[3] and [15]. The scattered signals were focused into a detector by a small area lens placed at 38° with respect to the Z axis.

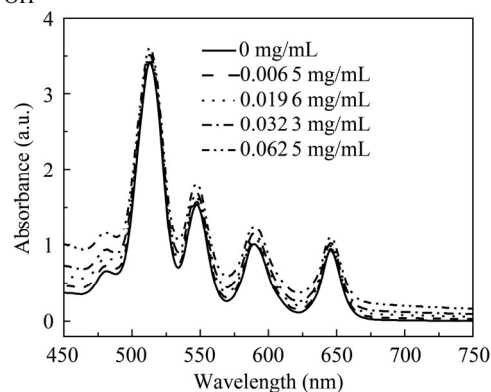
Fig.1 presents the absorption and fluorescence spectra of TPP and blends in DMF, respectively. As shown in Fig.1 (a) and (c), TPP and blends all show four characteristic Q bands of free porphyrins, locating at 513 nm, 547 nm, 589 nm and 646 nm, respectively. The additions of MWNTs-OH and GO do not affect the central wavelength and the width of Q bands, which indicates that the energy level of TPP is not changed by MWNTs-OH and GO, similar to the result of phthalocyanine-carbon nanotube blends<sup>[9]</sup>. The Soret band of TPP is not shown in Fig.1 due to the strong absorption of Soret band in the ultraviolet (UV) region which is beyond the ability of the spectrophotometer. As shown in Fig.1 (b) and (d), TPP and blends all exhibit two fluorescence bands around 657 nm and 718 nm, respectively. The excitation wavelength is 532 nm. The significant quenching of fluorescence in blends indicates non-radiative energy or electron transfer from TPP to MWNTs-OH and GO. Similar quenching is also observed in other covalent and non-covalent conjugated molecules-carbon nanomaterials systems<sup>[9-12]</sup>.



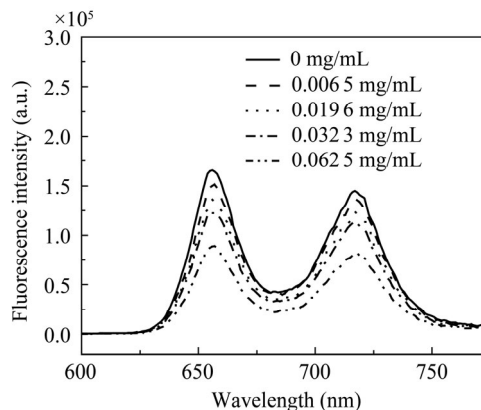
(a) Absorption spectra of blends with different concentrations of MWNTs-OH



(b) Fluorescence spectra of blends with different concentrations of MWNTs-OH



(c) Absorption spectra of blends with different concentrations of GO



(d) Fluorescence spectra of blends with different concentrations of GO

**Fig.1 The absorption and fluorescence spectra of TPP and TPP-oxygenated carbon nanomaterial blends with different concentrations of MWNTs-OH and GO in DMF (The concentration of TPP is 0.107 mg/mL.)**

Fig.2 shows the open-aperture Z-scan curves of TPP and TPP blended with MWNTs-OH dispersion at different on-focus input fluences, respectively. To evaluate and compare their optical nonlinearities, the effective nonlinear absorption coefficient  $\beta_{\text{eff}}$  is used. Using Crank-Nicholson finite difference method, we fit the Z-scan curves numerically and obtain the values of  $\beta_{\text{eff}}$ .

As shown in Fig.2, under three different input fluences of 0.602  $\text{J}\cdot\text{cm}^{-2}$ , 1.384  $\text{J}\cdot\text{cm}^{-2}$  and 1.986  $\text{J}\cdot\text{cm}^{-2}$ , the minimum normalized transmittances near focus ( $T_{\text{min}}$ ) of TPP

are 0.481, 0.460 and 0.447, and the  $\beta_{\text{eff}}$  values are 100 cm/GW, 49 cm/GW and 36 cm/GW, respectively. The  $T_{\text{min}}$  values of TPP-MWNTs-OH blend are 0.557, 0.439 and 0.327, and the  $\beta_{\text{eff}}$  values are 90 cm/GW, 75 cm/GW and 92 cm/GW, respectively. So it can be seen that as the input fluence increases,  $T_{\text{min}}$  of TPP decreases slightly, while its  $\beta_{\text{eff}}$  value reduces drastically. In general,  $\beta_{\text{eff}}$  value will increase as input fluence increases for NLS process, while it will keep unchanged for pure two-photon absorption process. The decrease of  $\beta_{\text{eff}}$  with fluence implies the RSA process<sup>[3]</sup>. For blend dispersion, as input fluence increases,  $T_{\text{min}}$  decreases drastically, while  $\beta_{\text{eff}}$  firstly decreases, and then increases. Decreasing  $T_{\text{min}}$  indicates strong OL effect, while the transition of  $\beta_{\text{eff}}$  values changing from decrease to increase indicates the dominant RSA from TPP moiety at lower fluence region and the dominant NLS from MWNTs-OH moiety at higher fluence region<sup>[3,15]</sup>, respectively. TPP-GO blend shows the similar behavior to TPP with the increase of fluence, but its  $\beta_{\text{eff}}$  value keeps smaller than that of TPP, due to the strong linear absorption but negligible optical nonlinearity of GO at these fluence ranges.

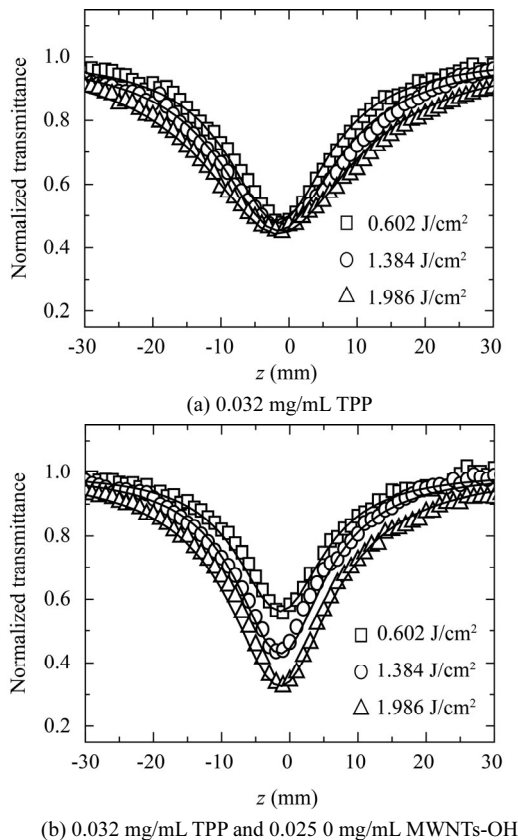


**Fig.2 Open-aperture Z-scan curves of TPP and TPP blended with MWNTs-OH dispersion under different input fluences on focus**

Fig.3 shows the open-aperture Z-scan curves of TPP blended with MWNTs-OH and GO dispersions, respectively. In blends with MWNTs-OH of 0 mg/mL, 0.012 2 mg/mL, 0.025 0 mg/mL and 0.048 8 mg/mL,  $T_{\text{min}}$  values

of the blends are 0.447, 0.357, 0.323 and 0.418, and  $\beta_{\text{eff}}$  values are 36 cm/GW, 68 cm/GW, 92 cm/GW and 66 cm /GW, respectively. As the concentration of MWNTs-OH increases,  $T_{\text{min}}$  firstly decreases, indicating the enhanced optical nonlinearity. However, if the concentration of MWNTs-OH is too high (0.048 8 mg/mL),  $T_{\text{min}}$  increases and  $\beta_{\text{eff}}$  becomes smaller, which indicates that optical nonlinearity can be weakened by strong linear absorption. In blend with GO of 0 mg/mL, 0.025 0 mg/mL, 0.041 1 mg/mL and 0.102 5 mg/mL,  $T_{\text{min}}$  values are 0.447, 0.475, 0.498 and 0.539, and  $\beta_{\text{eff}}$  values are 36 cm/GW, 32 cm/GW, 31 cm/GW and 29 cm/GW, respectively. As the concentration of GO increases,  $T_{\text{min}}$  increases and  $\beta_{\text{eff}}$  decreases, which is similar to TPP-MWNTs-OH blends with high concentration of MWNTs-OH. Since the optical nonlinearity and OL property of GO are too weak<sup>[15]</sup>, the optical nonlinearity of GO with concentrations of 0.025 0–0.102 5 mg/mL can not occur even at the fluence of 1.986 J·cm<sup>-2</sup>, so the addition of GO to TPP only enhances the linear absorption but leads to poor optical nonlinearity in low fluence region. So the moderate concentrations of MWNTs-OH and GO should be chosen.

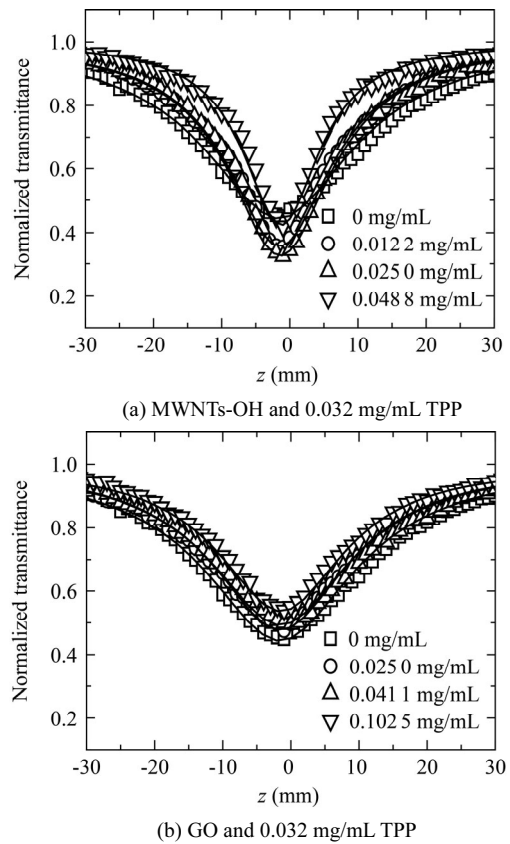


**Fig.3 Open-aperture Z-scan curves of TPP-MWNTs-OH and TPP-GO blends with different concentrations of MWNTs-OH and GO at on-focus input fluence of 1.986 J·cm<sup>-2</sup>**

For OL experiments, blends with moderate concentra-

tion ratio of TPP and carbon nanomaterial are firstly chosen (TPP: 0.032 mg/mL, MWNTs-OH: 0.025 0 mg/mL, GO: 0.025 0 mg/mL), and then the linear transmittances of all the samples are adjusted to be 75% at 532 nm. As shown in Fig.4(a), the normalized transmittance of MWNTs-OH is roughly constant when the input fluence is low, but when the input fluence exceeds  $0.838 \text{ J}\cdot\text{cm}^{-2}$ , the transmittance begins to decrease significantly. This indicates the NLS properties of MWNTs-OH<sup>[15]</sup>. Similar to MWNTs-OH, the transmittance of GO begins to decrease significantly when the fluence exceeds  $1.430 \text{ J}\cdot\text{cm}^{-2}$ . However, the transmittance of TPP begins to decrease even for the fluence exceeding  $0.1 \text{ J}\cdot\text{cm}^{-2}$ , but it decreases more slowly than those of MWNTs-OH and GO at high fluence region due to RSA saturation and/or thermal degradation. Different from individual MWNTs-OH, the transmittance of TPP blended with MWNTs-OH begins to decrease at a low fluence of  $0.243 \text{ J}\cdot\text{cm}^{-2}$ , and decreases drastically at high fluence region. Similarly, the transmittance of TPP-GO blend also begins to decrease at a low fluence of  $0.466 \text{ J}\cdot\text{cm}^{-2}$ , and decreases significantly at high fluence region. So the OL performance of blends is similar to that of TPP at low fluence region, while similar to the behavior of carbon nanomaterials at high fluence region, which indicates the complementary nonlinear optical mechanism of RSA and NLS from TPP and carbon nanomaterials, respectively.

From Fig.4(b), we can see NLS signal intensities follow a decreasing order of TPP-MWNTs-OH, MWNTs-OH, TPP-GO, GO and TPP, and the NLS can be attributed to nonlinear light scattering from ionized carbon microplasmas and solvent microbubbles<sup>[11-15]</sup>. Interestingly, as shown in Fig.4(a), the OL performance depends on the input fluence values due to the different nonlinear optical mechanisms. For example, in lower fluence region I (lower than  $1.430 \text{ J}\cdot\text{cm}^{-2}$ ), TPP shows the smallest normalized transmittance, and the OL performance follows a decreasing order of TPP, TPP-MWNTs-OH, TPP-GO, MWNTs-OH and GO. It can be attributed to the dominant RSA from TPP moiety and negligible NLS at the lower fluence region I. In high fluence region III (higher than  $9.37 \text{ J}\cdot\text{cm}^{-2}$ ), TPP shows the largest normalized transmittance, and the OL performance follows a decreasing order of TPP-MWNTs-OH, MWNTs-OH, TPP-GO, GO and TPP. The two blends exhibit stronger OL than that of individual materials. The enhanced OL effect may arise from not only the combination of RSA and NLS, but also the photoinduced electron or energy transfer from electron donor of TPP to acceptor of MWNTs-OH (or GO)<sup>[11,12]</sup>, respectively. TPP-MWNTs-OH blend exhibits the stronger OL effect than TPP-GO blend due to the stronger NLS of MWNTs-OH. In the medium fluence region II, as the input fluence increases, the order varies due to the different change trends of RSA and NLS.

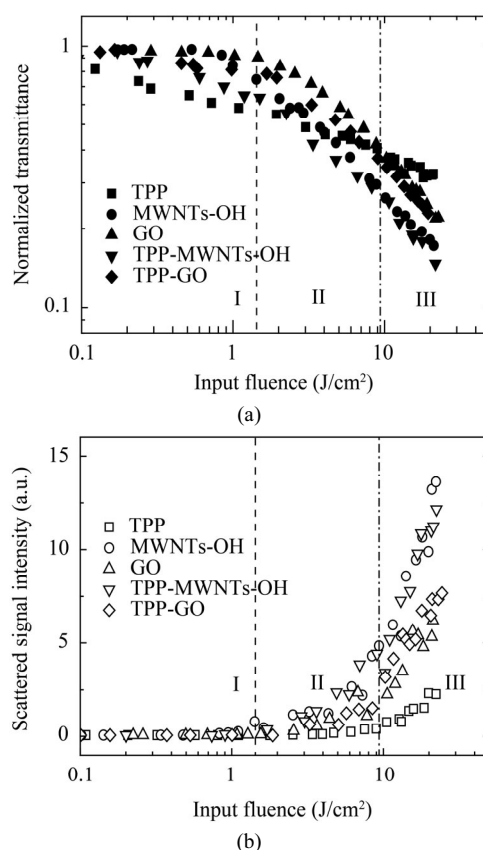


**Fig.4 (a) Normalized transmittance and (b) scattered signal intensity as a function of the input fluence for TPP, MWNTs-OH, GO and their blends with the same linear transmittance of 75% at 532 nm**

In conclusion, the optical nonlinearity and OL property of TPP can be improved or tuned by adding MWNTs-OH and GO due to the complementary nonlinear optical mechanism and possible photoinduced electron or energy transfer mechanism between TPP moiety and oxygenated carbon nanomaterials. The preparation of blend system with complementary nonlinear optical mechanisms may be a better way to improve or tune the OL property of materials.

## References

- [1] P. Aloukos, I. Papagiannouli, A. B. Bourlinos, R. Zboril and S. Couris, *Optics Express* **22**, 12013 (2014).
- [2] M. H. Wang, G. P. Zhu, H. Q. Zhu, Y. F. Ju, R. D. Ji and L. H. Fu, *Optoelectronics Letters* **10**, 1 (2014).
- [3] X. L. Zhang, X. D. Chen, X. C. Li, C. F. Ying, Z. B. Liu and J. G. Tian, *Journal of Optics* **15**, 055206 (2013).
- [4] K. Jiang, J. J. Xie, L. M. Zhang, D. J. Li, J. J. Xie and A. Yury, *Journal of Optoelectronics-Laser* **24**, 903 (2013). (in Chinese)
- [5] T. Qin, H. B. Liu, X. X. Deng and X. W. Zheng, *Journal of Optoelectronics-Laser* **25**, 1466 (2014). (in Chinese)
- [6] É. M. Ní Mhuircheartaigh, S. Giordani and W. J. Blau, *The Journal of Physical Chemistry B* **110**, 23136 (2006).

- [7] X. Sun, R. Q. Yu, G. Q. Xu, T. S. A. Hor and W. Ji, *Applied Physics Letters* **73**, 3632 (1998).
- [8] J. Wang, Y. Hernandez, M. Lotya, J. N. Coleman and W. J. Blau, *Advanced Materials* **21**, 2430 (2009).
- [9] J. Wang and W. J. Blau, *Chemical Physics Letters* **465**, 265 (2008).
- [10] X. Zhao, X. Q. Yan, Q. Ma, J. Yao, X. L. Zhang, Z. B. Liu and J. G. Tian, *Chemical Physics Letters* **577**, 62 (2013).
- [11] A. J. Wang, L. L. Long, W. Zhao, Y. L. Song, M. G. Humphrey, M. P. Cifuentes, X. Z. Wu, Y. S. Fu, D. D. Zhang, X. F. Li and C. Zhang, *Carbon* **53**, 327 (2013).
- [12] Z. B. Liu, Z. Guo, X. L. Zhang, J. Y. Zheng and J. G. Tian, *Carbon* **51**, 419 (2013).
- [13] Q. Wang, Y. J. Qin, Y. J. Zhu, X. Huang, Y. X. Tian, P. Zhang, Z. X. Guo and Y. L. Wang, *Chemical Physics Letters* **457**, 159 (2008).
- [14] N. Liaros, P. Aloukos, A. Kolokithas-Ntoukas, A. Bakandritsos, T. Szabo, R. Zboril and S. Couris, *The Journal of Physical Chemistry C* **117**, 6842 (2013).
- [15] X. L. Zhang, Z. B. Liu, X. Q. Yan, X. C. Li, Y. S. Chen and J. G. Tian, *Journal of Optics* **17**, 015501 (2015).
- [16] H. A. Becerril, J. Mao, Z. F. Liu, R. M. Stoltenberg, Z. N. Bao and Y. S. Chen, *ACS Nano* **2**, 463 (2008).
- [17] M. Sheik-Bahae, A. A. Said, T. H. Wei, D. J. Hagan and E. W. Van Stryland, *IEEE Journal of Quantum Electron.* **26**, 760 (1990).